Available online at www.sciencedirect.com
SCIENCE DIRECT
Polymer 47 (2006) 2156–2162
polymer
www.elsevier.com/locate/polymer

The influence of drawing temperature on mechanical properties and organization of melt spun polyethylene solid-state drawn in the pseudo-affine regime

Xin Hu [a], Ben Alcock [b,d], Joachim Loos [b,c,d,*]

[a] School of Chemistry and Chemical Technology, Shanghai Jiao Tong University, Shanghai 200240, People's Republic of China
[b] Laboratory of Polymer Technology, Eindhoven University of Technology, 5600 MB Eindhoven, The Netherlands
[c] Laboratory of Materials and Interface Chemistry, Department of Chemical Engineering and Chemistry, Eindhoven University of Technology, P.O. Box 513, Helix STO 0.41, 5600 MB Eindhoven, The Netherlands
[d] Dutch Polymer Institute, Eindhoven University of Technology, 5600 MB Eindhoven, The Netherlands

Received 14 November 2005; received in revised form 8 January 2006; accepted 13 January 2006

Abstract

Mechanical properties of high density polyethylene (HDPE) solid-state drawn with fixed draw ratio at different temperatures in a fiber/tape spin line were investigated. All drawing experiments were performed in the pseudo-affine regime, i.e. no effective relaxation of the molecules occurs during drawing. For such conditions, the Young's modulus is uniquely determined by the applied draw ratio. The general appearance of the stress–strain behavior of drawn HDPE, and in particular its yield strength, however, is strongly influenced by the stretching temperature applied. For a fixed draw ratio, a significant drop in yield stress can be observed with decreasing drawing temperature. Characterization of structure and organization of the solid-state drawn HDPE was performed using various analytical techniques, such as wide-angle X-ray diffraction (WAXD) and differential scanning calorimetry (DSC). It is proposed that solid-state drawing at temperatures above the α-relaxation temperature results in relative large crystals so that corresponding tapes show a high yield point. Drawing at low temperatures below the α-relaxation temperature of PE, however, causes formation of small or imperfect crystals that can be destructed at low stress (low yield point), which is a preferable start situation for a second solid-state drawing step in a multiple drawing process.

Keywords: Polyethylene; Solid–state drawing; Structure–property relation

1. Introduction

Stiffness and strength of bulk polymers are insufficient for many applications due to the random orientation of the polymer molecules, and in case of semi-crystalline polymers such as polyethylene or polypropylene the random orientation of crystals. To overcome this limitation, it has been appreciated since a long time that molecular orientation induced by fiber spinning, mainly in combination with subsequent solid-state drawing, can enhance the mechanical properties of polymers [1]. To gain fibers offering high stiffness and strength, successfully the process of gel-spinning followed by solid-state drawing has been demonstrated and commercialized for ultra-high molecular weight polyethylene (UHMWPE) [2,3]. Reduction of entanglement density in a gel precursor for subsequent solid-state drawing with high draw ratios up to about 100 times is the key feature of this process towards fibers with ultimate stiffness and strength. However, because of low polymer concentrations in the solution throughput is limited and solvent recycling is a serious issue, which make this process expensive.

On the other hand, melt-spinning followed by solid-state drawing as a low cost process allows, in general, only low draw ratios, and achievable mechanical properties are much lower when compared with gel-spinning. To overcome these limitations, at least in part, multi-stage drawing procedures were introduced [4–8]. In this respect, the influence of drawing conditions on the mechanical properties, the effect of molecular weight and molecular weight distribution as well as the initial morphology on mechanical properties has been

* Corresponding author. Address: Department of Chemical Engineering and Chemistry, Eindhoven University of Technology, P.O. Box 513, Helix STO 0.41, 5600 MB Eindhoven, The Netherlands. Tel.: +31-40-2473034
E-mail address: j.loos@tue.nl (J. Loos).

0032-3861/$ - see front matter © 2006 Elsevier Ltd. All rights reserved.
doi:10.1016/j.polymer.2006.01.046

investigated seriously. Less attention has been paid to the effect of drawing temperature used on the final mechanical properties [9,10]. It is commonly concluded that for pseudo-affine drawing conditions, i.e. as long as molecular relaxation can be avoided, mechanical properties of solid-state drawn fibers or tapes uniquely depend on the draw ratio applied [11,12]. Mainly for high temperatures with effective relaxation processes during drawing significant change of mechanical properties is observed.

In case of isotactic polypropylene (iPP), we have shown that the mechanical properties of fibers and tapes can be tailored by the drawing temperature applied, especially for low temperatures in the pseudo-affine drawing regime [13]. For a fixed draw ratio, a significant drop in yield stress can be observed with lowering the drawing temperature. This behavior is explained by formation of small crystals in the mesomorphic phase, which subsequently can be destructed at low stress (low yield point). In the present study, we like to report that also high density polyethylene (HDPE) tapes solid-state drawn at temperatures below their α-relaxation temperature of about 80 °C have a substantially lower yield stress when compared with tapes drawn at higher temperatures at the same draw ratio. The origin of this behavior will be discussed based on wide-angle X-ray diffraction (WAXD), DSC and free shrinkage experiments. Because of their low yield stress, such tapes easily can be deformed again in a potential second step of a multiple drawing process so that high total draw ratios can be reached.

2. Experimental section

The high density polyethylene homopolymer (M30053s) used was kindly supplied by Sabic, The Netherlands. The material has a density of 953 kg/m^3 (ISO 1183) and melt flow rate (MFR) of 4 g/10min (ISO 1133).

The tapes were prepared using a tape manufacturing line consisting of single screw extruder, nozzle, chill roll, godet, oven, and winder. The godet speed is referred to the speed at which the tape enters the oven. The winder speed determines the velocity at which the tape comes out of the oven. The draw ratio (λ) within the oven is determined by the ratio of winder speed and godet speed. Fig. 1 shows a sketch of the fiber spinning and solid-state drawing line. The presented results are based on tapes that are solid-state drawn to the ratios $\lambda = 3$ and 5. The godet had a speed of 10 m/min, and the corresponding velocity of the winder was 30 and 50 m/min, respectively. While all processing parameters, especially the output of the extruder, were kept constant, the oven temperature was varied from 20 to 120 °C.

The mechanical properties of the drawn tapes were measured at room temperature using a Zwick 100 tensile tester equipped with an extensometer, force reducing clamps and a load-cell of 500 N. The tensile tests were carried out with tapes of initial gauge length of 150 mm and at a crosshead speed of 0.2 mm/s. Force–elongation curves were recorded on a central section of the tapes with a length of 50 mm. A pre-load of about 0.5 N was applied on the samples. A set of 10 tensile tests was performed on each tape.

To relate the measured tensile force to the cross-section area, and thus to be able to calculate the stress applied to the tapes, thickness and width of the drawn tapes were measured. The thickness and width were determined with a digital micrometer. For both dimensions, the average of 10 independent measurements, spread over a tape length of 10 m, was taken as the representative value. The instrument has an accuracy of 1% of the measured value.

Wide-angle X-ray diffraction (WAXD) patterns of the tapes were recorded with a two-dimensional area detector, general area detector diffraction system (GADDS), with an exposure time of 5 min. A Bruker D8discover X-ray generator working at 40 kV and 40 mA created the X-ray beam. The Cu K_α radiation had an average wavelength of 1.542 Å, while the Cu K_β radiation was eliminated by a Ni filter.

Differential scanning calorimetry (DSC) was performed on 5 mg samples of the tapes, using a TA Instruments DSC Q1000 differential scanning calorimeter. Samples were heated in the DSC from ambient temperature to 180 °C at 10 °C min^{-1}. To determine the melting temperature as well as heat of fusion of the oriented tapes, only the first heating cycle was analyzed. The crystallinity χ was calculated using Eq. (1), where ΔH is the heat of fusion of the sample and ΔH° is heat of fusion of a perfect orthorhombic polyethylene crystal

$$\chi = \Delta H/\Delta H^\circ \quad (1)$$

the value of ΔH° was taken as 289 J/g [14]. In these calculations it was assumed that for any other phases present (e.g. triclinic) the heat of fusion is equal to that of the orthorhombic form.

To assess the free shrinkage of solid-state drawn polyethylene, tapes with a length of 0.5 m were hung for 1 h in a

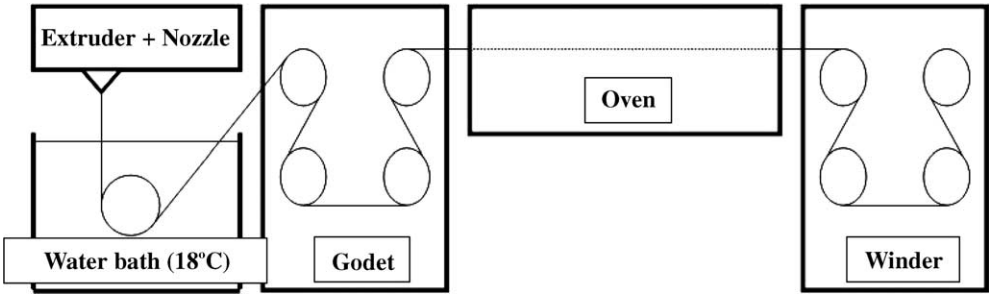

Fig. 1. Sketch of the fiber spinning and solid-state drawing line.

preheated, circulating air oven controlled by an internal thermostat and monitored by an independent thermometer. The air temperature was constant, and uniform (±2 °C) within the oven. Total shrinkage is defined as fraction of initial sample length remaining after exposure to elevated temperature.

3. Results

A set of stress–strain curves of HDPE tapes solid-state drawn at different temperatures for $\lambda = 3$ is shown in Fig. 2. All tapes exhibit the same average stiffness of about 2 GPa, independent of the drawing temperature. The constancy of the stiffness is in agreement with the Irvine–Smith model, which predicts that the Young's modulus uniquely depends on the applied network draw ratio for the pseudo-affine deformation regime; non-affine deformation of PE is observed, for our setup, only for temperatures above 120 °C. While the drawing temperature does not influence the stiffness, a significant drop in yield stress and stress at break can be observed by lowering the drawing temperature from 120 to 20 °C: drawing at 120 °C results in tapes having a yield stress of about 110 MPa and stress at break of about 170 MPa, whereas, the yield stress and stress at break for tapes drawn at 20 °C is about 60 and 110 MPa, respectively. All tapes show homogeneous deformation behavior rather then necking. An overview of average values for stiffness and yield stress is given in Table 1.

Tapes drawn at different temperature for $\lambda = 5$ show a similar behavior (Fig. 3). All tapes exhibit the same average stiffness of about 4.5 GPa, independent of the drawing temperature while the yield stress decrease from 190 to 150 MPa when decreasing the drawing temperature form 120 to 20 °C (Table 1). Again, all tapes show homogeneous deformation behavior. For higher draw ratios, the influence of the drawing temperature on the mechanical behavior of the tapes becomes less and less pronounced.

To prove whether the observed mechanical behavior is caused by inadequacies in the drawing process, the measured thickness and width of the drawn tapes were related to the theoretical values calculated for a purely uniaxial deformation

Table 1
Average Young's modulus (E) and average yield stress (σ) of HDPE tapes solid-state drawn at various temperatures (T_{draw})

T_{draw} (°C)	$\lambda = 3$		$\lambda = 5$	
	E (GPa)	σ (MPa)	E (GPa)	σ (MPa)
20	2.0±0.17	60±1	4.5±0.12	150±2
80	2.0±0.11	80±3	4.5±0.16	170±3
120	2.0±0.05	110±2	4.5±0.09	190±1

under the assumption of constant volume ($\lambda_L \lambda_T \lambda_W = 1$) and isotropic drawing behaviour in the lateral dimensions ($\lambda_T = \lambda_W$); L, T and W represent length, thickness and width of the tape, respectively. The theoretical thickness (d) for a certain draw ratio results from

$$d = \frac{d_0}{\sqrt{\lambda}} \tag{2}$$

where d_0 represents the thickness of the tape before drawing. The same formula can be used to calculate the theoretical width (w) by replacing d and d_0 by w and w_0, respectively. To generate theoretical curves for thickness/width vs. draw ratio, which are independent from the dimensions of the precursor tape, the values for d and w were normalized by dividing by d_0 and w_0, respectively. The authors are aware of the slight inaccuracy for theoretical thickness and width values obtained by the assumption of constant volume. More precise is the assumption of constant mass, which takes in account changes in density while drawing. However, the error is assumed to be below 2%.

As can be seen from Fig. 4, measured thickness and width of tapes having different draw ratios produced in the above described manufacturing line fit very well to the theoretical curve and are independent of drawing temperature. Data points up to draw ratios of 7 refer to the average of 30 independent measurements, 10 measured for each drawing temperature of 20, 80, and 120 °C, respectively. This implies that the prepared tapes are uniaxially deformed while drawing and that the draw ratio is uniquely determined by the ratio of winder speed and godet speed.

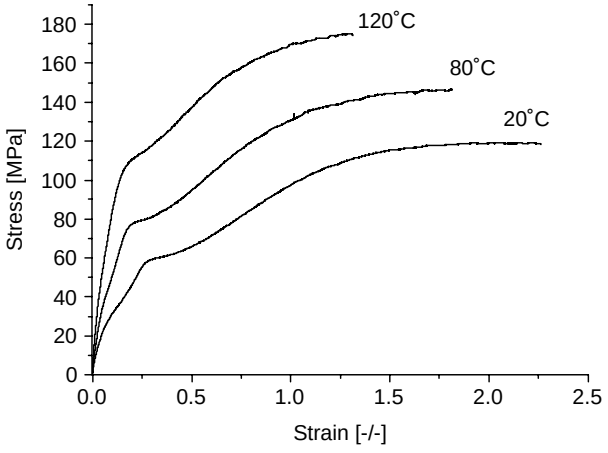

Fig. 2. Stress–strain plots of HDPE tapes, solid-state drawn at different drawing temperatures with draw ratio $\lambda = 3$.

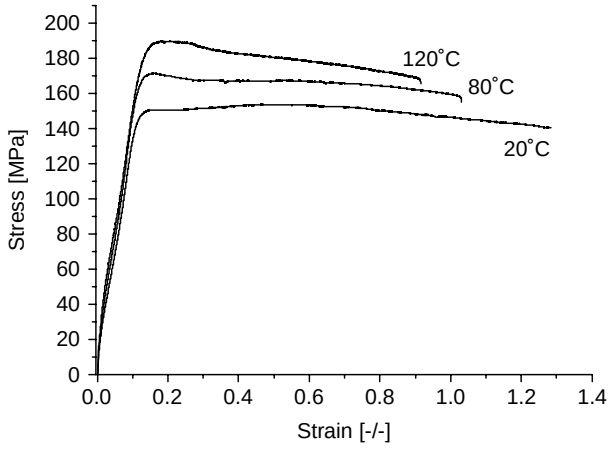

Fig. 3. Stress–strain plots of HDPE tapes, solid-state drawn at different drawing temperatures with draw ratio $\lambda = 5$.

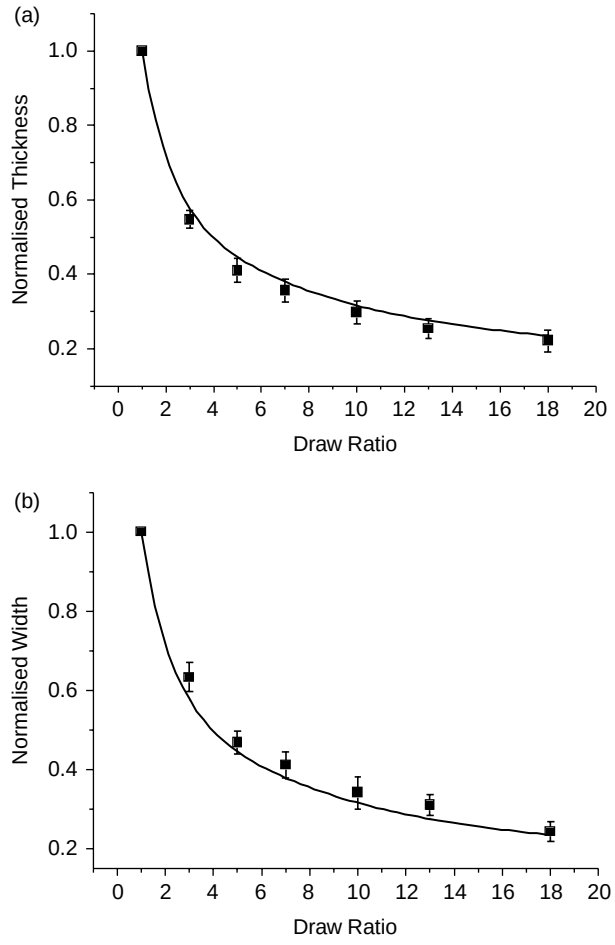

Fig. 4. Normalized thickness/width of drawn tapes vs. draw ratio: (a) normalized thickness and (b) normalized width; data points up to draw ratios of seven refer to the average of 30 independent measurements, 10 measured for each drawing temperature of 20, 80 °C, and 120°, respectively; solid lines refer to theoretical data.

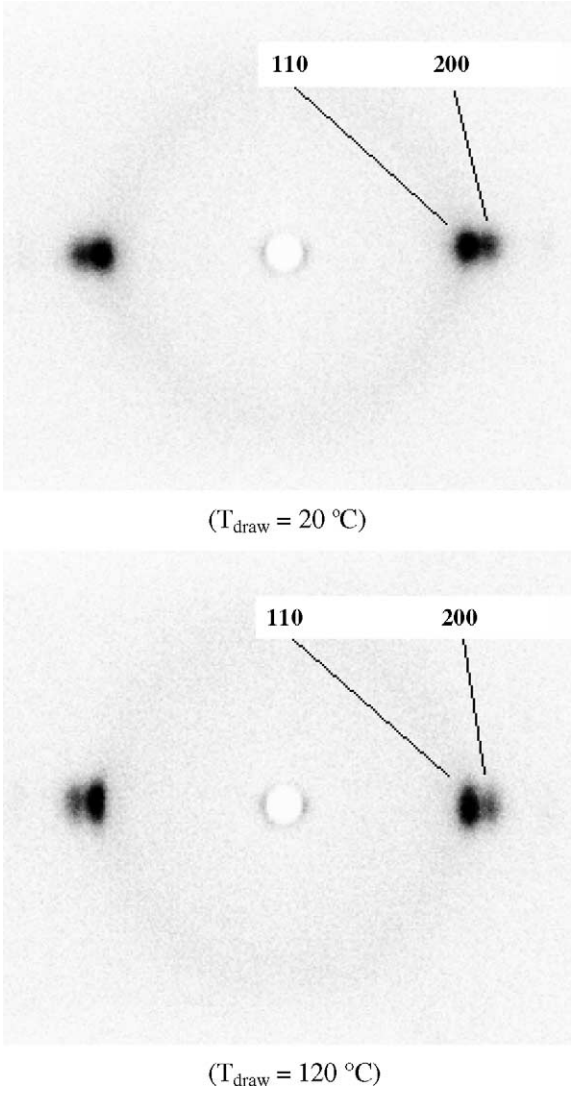

Fig. 5. Wide-angle X-ray diffraction patterns of tapes drawn at 20 and 120 °C, draw ratio is $\lambda = 5$.

To investigate the influence of drawing temperature on crystallinity and organization of the HDPE tapes, X-ray, DSC and free shrinkage experiments were performed. Because of similarity of the behavior only results from tapes solid-state drawn with $\lambda = 5$ are presented. Fig. 5 shows wide-angle X-ray diffraction patterns of tapes drawn at 20 and 120 °C, respectively. For both tapes, the occurrence of sharp reflections is a clear indication for a fiber pattern. Tapes drawn at 120 °C possess a smaller radial peak width compared to those drawn at 20 °C. This can be seen from the (110) peak in the diffraction pattern. At the drawing temperature of 120 °C one can distinguish between these peaks, while they are blurred in the pattern for the drawing temperature of 20 °C. The smaller radial peak width reflects a larger crystal size and/or higher crystal perfection in the case of the higher drawing temperature. From the patterns one can also observe that the peaks have different arc lengths depending on the drawing temperature. The arc length can be associated with the broadness of the orientation distribution of the crystals having orthorhombic crystal unit cell. For tapes drawn at 120 °C the crystals are less aligned in the drawing direction as compared to the tapes drawn at 20 °C.

Fig. 6 shows plots of one-dimensional intensity distributions as a result of an integration of two-dimensional X-ray images along the azimuthal angle. The (110) peak width is clearly wider for the tape drawn at 20 °C when compared with tapes drawn at 120 °C. In order to quantify this, the full width at half maximum (FWHM) of the radial width of the (110)-reflection was determined. In Fig. 7 the inverse of the determined FWHM-value is shown as a function of the post drawing temperature. It can be seen that the inverse FWHM of the radial width of the (110)-reflection increases almost steady with increasing post drawing temperature. Since the radial peak width is inversely proportional to the size and/or perfection of crystals, this result indicates an increasing coherence of the crystals in (110)-direction with increasing post drawing temperature, i.e. larger crystal size and/or higher crystal perfection.

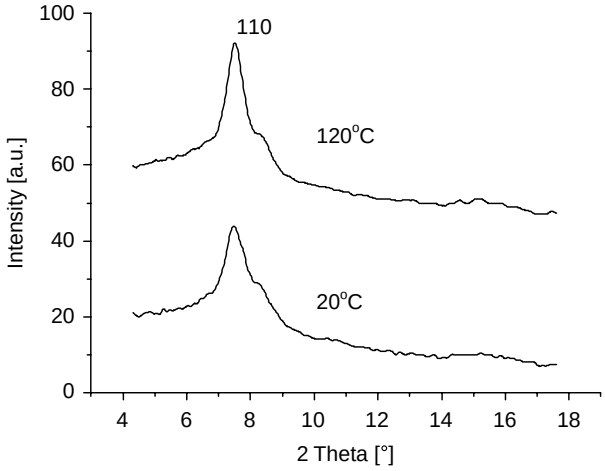

Fig. 6. One-dimensional intensity scans integrated along the azimuthal angle of the two-dimensional X-ray pattern of Fig. 4, drawing temperatures as indicated in the diagram, draw ratio is $\lambda = 5$.

Fig. 8 shows the DSC curves of the samples prepared at different drawing temperature. The width of the DSC peaks becomes narrower while increasing the drawing temperature, indicating the crystal size within the samples becomes more homogeneous. Moreover, the peak melting temperature increases with drawing temperature (Fig. 9). Since the melting temperature can be related to the lamellar thickness and/or crystal size and perfection, it seems reasonable to say that larger crystal size and/or higher crystal perfection can be found with increasing the drawing temperature. However, the authors are aware that during DSC measurement samples tend to reorganize, and thus the obtained melting characteristics may not reflect the initial organization of the tapes. Fig. 10 shows the crystalinity of the samples with increased drawing temperature as calculated from heat of fusion measurement by DSC. The crystallinity increases steadily with increasing the drawing temperature.

Free shrinkage experiments were performed to investigate changes of the organization of the amorphous phase depending on the drawing temperature. Fig. 11 shows the degree of shrinkage after exposure to various oven temperatures for tapes drawn at different temperatures. In general, the shrinkage behavior is non-linear and increases with increasing oven temperature; however, shrinkage is less pronounced for tapes drawn at high temperatures.

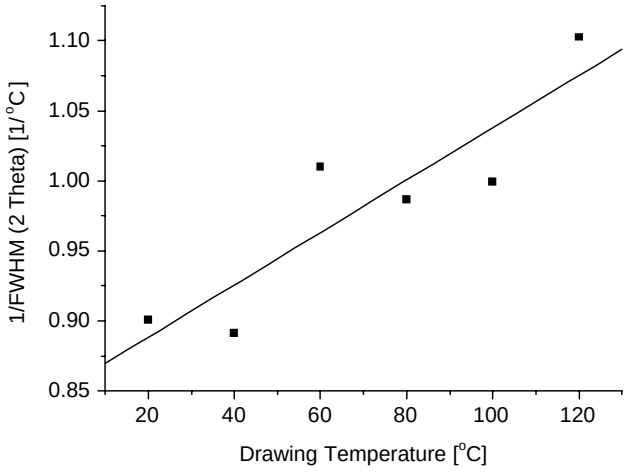

Fig. 7. Inverse of the 2Θ-FWHM values as a function of the post drawing temperature, draw ratio is $\lambda = 5$.

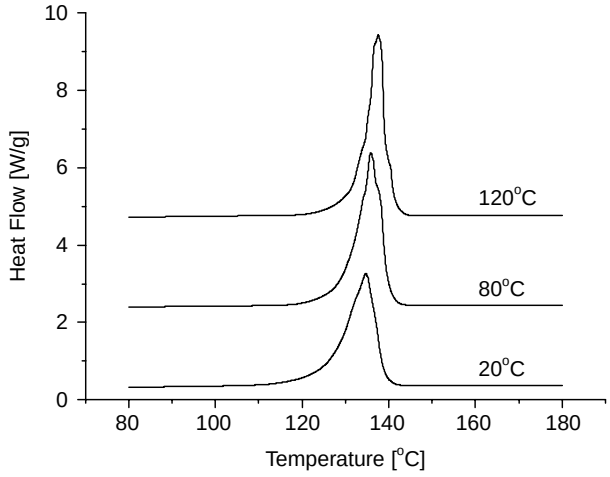

Fig. 8. DSC curves for tapes drawn at various drawing temperatures, draw ratio is $\lambda = 5$.

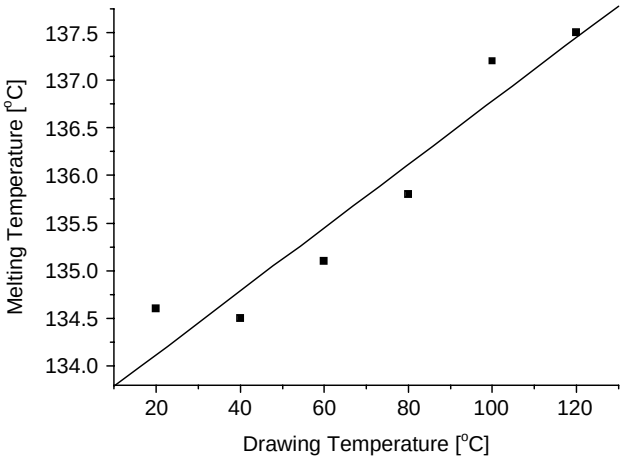

Fig. 9. Melting temperature for tapes drawn at various drawing temperatures, draw ratio is $\lambda = 5$.

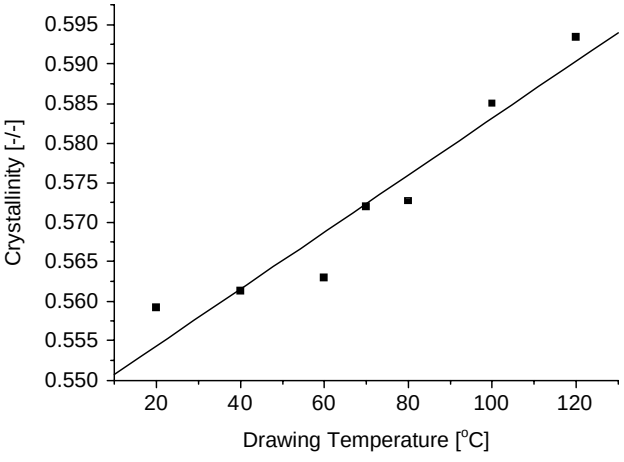

Fig. 10. Crystalinity vs. drawing temperature, draw ratio is $\lambda = 5$.

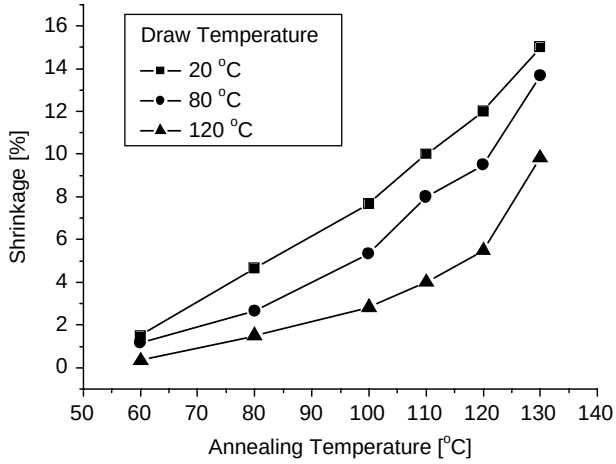

Fig. 11. Relative shrinkage vs. annealing temperature for tapes drawn at various drawing temperatures.

Table 2
Summary of properties influenced by the solid-state drawing temperature applied

	Low drawing temperature	High drawing temperature
Crystallinity	▼	▲
Melting temperature	▼	▲
Orientation distribution	▲	▼
Shrinkage	▲	▼

▼/▲, Property decreases/increases.

4. Discussion

HDPE tapes show differences in their overall tensile behavior depending on the solid-state drawing temperature applied. While the measured stiffness is uniquely determined by the draw ratio, which means that in our experiments drawing was performed always in the pseudo-affine regime, the overall mechanical behavior and especially the yield stress is strongly influenced by the drawing temperature. Wide-angle X-ray diffraction measurements, differential scanning calorimetry heating scans and free shrinkage measurements reveal that the drawing temperature has an enormous influence on organization and properties of solid-state drawn HDPE tapes, even for pseudo-affine conditions. As described in the results part, larger crystal sizes and/or higher crystal perfection, higher melting temperature, lower crystal orientation as well as small free shrinkage can be achieved in the case of applying high drawing temperatures well above the α-relaxation temperature of PE, i.e. a temperature above which molecule stems in a crystal have higher mobility. In contrast, drawing below α-relaxation temperature resulted in smaller crystal sizes and/or less crystal perfection, lower melting temperature, high crystal orientation and large free shrinkage. However, exact determination of the α-relaxation temperature is difficult, and the value of 80 °C should be only an indication. A summary of this behavior is shown in Table 2.

Before drawing in the oven, all tapes possess the same morphology consisting of slightly oriented lamellar crystals embedded in a possibly slightly oriented amorphous matrix, both caused by the pre-orientation during extrusion and tape shaping (Fig. 12). Subsequently, the tape is solid-state deformed in the oven by applying stress to the tape induced via the speed difference between godet and winder. At the beginning, the deformation causes mainly stretching of the amorphous phase until the local stress results in destruction of the crystals. For low drawing temperature below the α-relaxation temperature the crystals fragment in small sections upon drawing. Because for such conditions stem

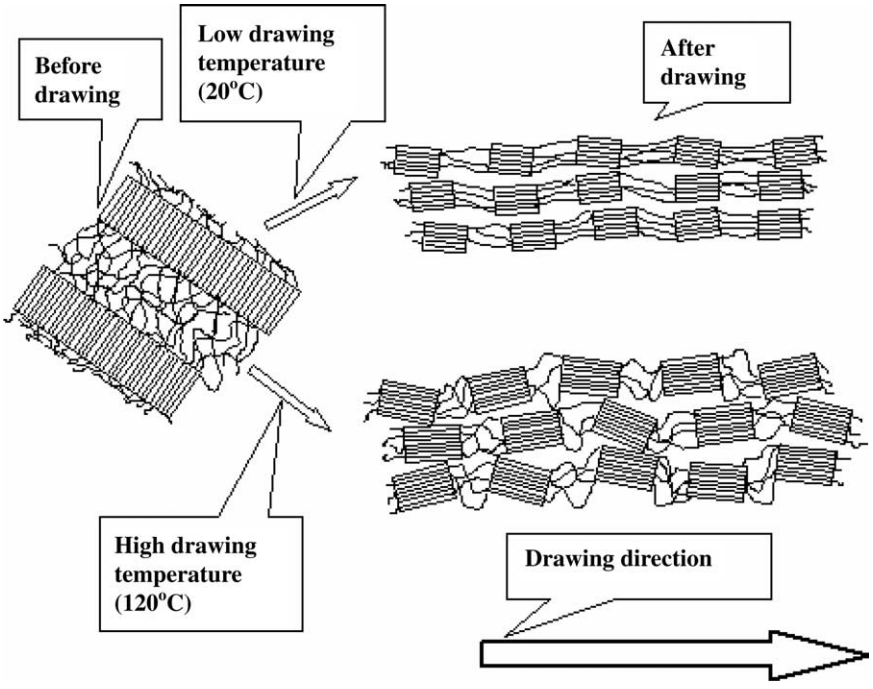

Fig. 12. Sketch visualizing the morphologies formed during solid-state drawing at different temperatures.

mobility in the crystals is negligible, and no effective molecular relaxation of the amorphous phase takes place on the time scale of the deformation process, crystal thickening or healing does not occur and both crystal as well as amorphous phases stay highly oriented. A sketch of such morphology can be seen in Fig. 12, top part.

Another indication for the presence of small and/or imperfect crystals in tapes solid-state drawn at low temperatures comes from WAXD data presented in Figs. 5–7, which show large widths of the crystal reflections. Further, the arc length of the reflections is small (Fig. 5), which is an indication for high degree of orientation of the crystals. Moreover, the pronounced shrinkage of the tapes in the annealing experiment (Fig. 11) point to a high degree of molecular orientation present in the amorphous phase.

Assuming such organization for tapes solid-state drawn at low temperatures, the small and/or imperfect crystals can be easy destructed, which is reflected by the low yield stress observed during tensile test (Figs. 2 and 3). For a particular crystal, yield stress increases with crystal thickness, which is related to the number of van der Waals bonds between neighboring chain stems that increases with crystal thickness and perfection. Such small and/or imperfect crystals can be identified also from DSC measurements because of their low melting temperatures and low crystallinity (Figs. 8–10).

For high drawing temperatures, fragmentation of crystals during drawing follows a similar route as described above, and still no effective relaxation happens. However, upon drawing above the α-relaxation temperature of PE, crystals can be easily destructed and recrystallize. Moreover, subsequent to drawing annealing of the drawn tape takes place in the oven, which enables relaxation of the amorphous phase and crystal thickening and/or healing. The first is seen from the reduced shrinkage during annealing experiments (Fig. 11) and the broader distribution of the crystal orientation (WAXD data of Fig. 5), the latter from the small azimuthal width of the crystalline WAXD peaks (Figs. 5–8) and the higher melting temperature and crystallinity as obtained from DSC measurements (Figs. 9 and 10). As a result of such tape organization, tapes drawn at high temperatures have higher yield strength. A sketch of the organization formed during drawing at high temperatures can be seen in Fig. 12, bottom part.

For higher draw ratios, the observed influence of the drawing temperature on the mechanical behavior of the tapes becomes less and less pronounced, because, possibly, overall orientation of crystal and amorphous phases is high and the fibrilar crystals formed are such large for all drawing temperatures that their destruction happens at similar yield stresses.

5. Conclusions

For pseudo-affine conditions, i.e. no effective relaxation of the molecules occurs during drawing, the effect of the solid-state drawing temperature applied on the mechanical properties as well as on organization of HDPE tapes has been described. It could be shown that the stiffness of the samples depends only on the applied draw ratio. In contrast, the overall mechanical behavior, and especially yield stress is strongly influenced by the drawing temperature applied. For a fixed draw ratio, a significant drop in yield stress can be observed with lowering the drawing temperature. These differences in mechanical behavior can be explained by drawing temperature dependent variations of the sample organization, which is displayed by differences in crystallinity, crystal size, and orientation of the crystal and amorphous phases. Tapes prepared at high temperatures above the α-relaxation temperature of PE contain larger crystals, which are formed during drawing and subsequent annealing in the oven. These tapes show a high yield stress. On the other hand, tapes prepared at temperatures below the α-relaxation temperature contain of highly oriented but small and/or imperfect crystals in a constrained amorphous phase, and have rather low yield stress. As consequence, these tapes can be easily deformed in a second drawing step of a multiple drawing process.

Acknowledgements

The authors are thankful to the Dutch Polymer Institute (DPI, projects 462 and 505) for support. The authors also thank Björn Tuerlings, Joost Valeton and Marco Hendrix for their support for tensile measurement, DSC measurement and X-ray investigations. X.H. would like to thank European Union for finial support through the Asia-Link Programme ASI/B7-301/98/679-32 and DSM for technical support.

References

[1] Ziabicki A. Fundamentals of fibre formation. London: Wiley; 1976.
[2] Smith P, Lemstra PJ. J Mater Sci 1980;15:505.
[3] Ward IM, Ciferri A. Ultra-high modulus polymers. London: Applied Science Publishers; 1979.
[4] Andreassen E, Myhre OJ, Hinrichsen EL, Grastad K. J Appl Polym Sci 1994;52:1505.
[5] Amornsakchai T, Cansfield DLM, Jawad SA, Pollard G, Ward IM. J Mater Sci 1993;28:1689.
[6] Ward IM. Plast Rubber Compos Process Appl 1993;19:7.
[7] Hallam MA, Cansfield DLM, Ward IM, Pollard G. J Mater Sci 1986;21:4199.
[8] Smith P, Lemstra PJ, Pijpers JPL. J Polym Sci, Polym Phys Ed 1982;20:2229.
[9] Balta Calleja FJ, Peterlin A. J Mater Sci 1969;4:722.
[10] Glenz W, Peterlin A, Wilke W. J Polym Sci, Polym Phys Ed 1971;9:1243.
[11] Irvine PA, Smith P. Macromolecules 1986;19:240.
[12] Dirix Y, Tervoort TA, Bastiaansen CWM, Lemstra PJ. J Textile Inst 1995;86:314.
[13] Schimanski T, Peijs T, Lemstra PJ, Loos J. Macromolecules 2004;37:1810.
[14] http://web.utk.edu/~athas/databank/intro.html.